Mizuno Supplementary Figure S1.

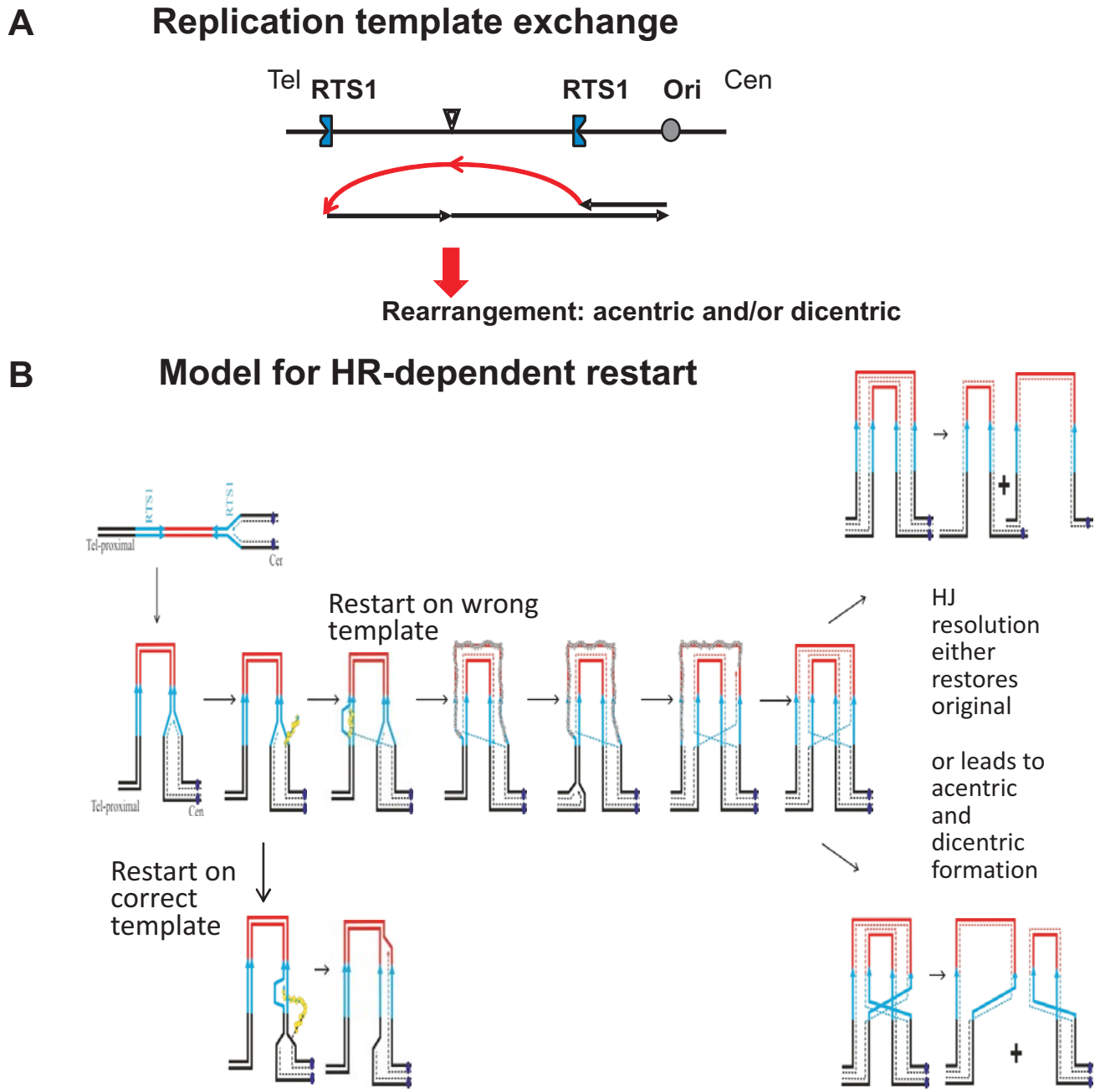

Figure S1: Models of replication restart leading to template exchange. (A) Use of an ectopic sequence to template HR-dependent replication restart leads to rearrangements generating acentric and dicentric chromosomes. (B) Our model suggests that the nascent strand becomes single stranded behind a collapsed fork, associates with HR proteins and subsequently anneals with the correct template to resume replication (bottom panels). However, if a DNA sequence homologous to the collapse site is nearby, an erroneous invasion of the nascent strand can occur, causing template exchange such that replication reinitiates ectopically. In these situations the restarted fork exchanges templates, resulting in single (shown) or double Holliday Junctions (HJs) (not shown) between the RTS1 sequences. Resolution of a single HJ can occur in 2 planes: resolution in one plane results in two identical sister chromatids, but resolution in the second plane generates inverted chromosomal fusions manifesting as acentrics and dicentrics. Double HJs resolution can additionally lead to inversion of the intervening ura4 sequence.

Mizuno Supplementary Figure S2.

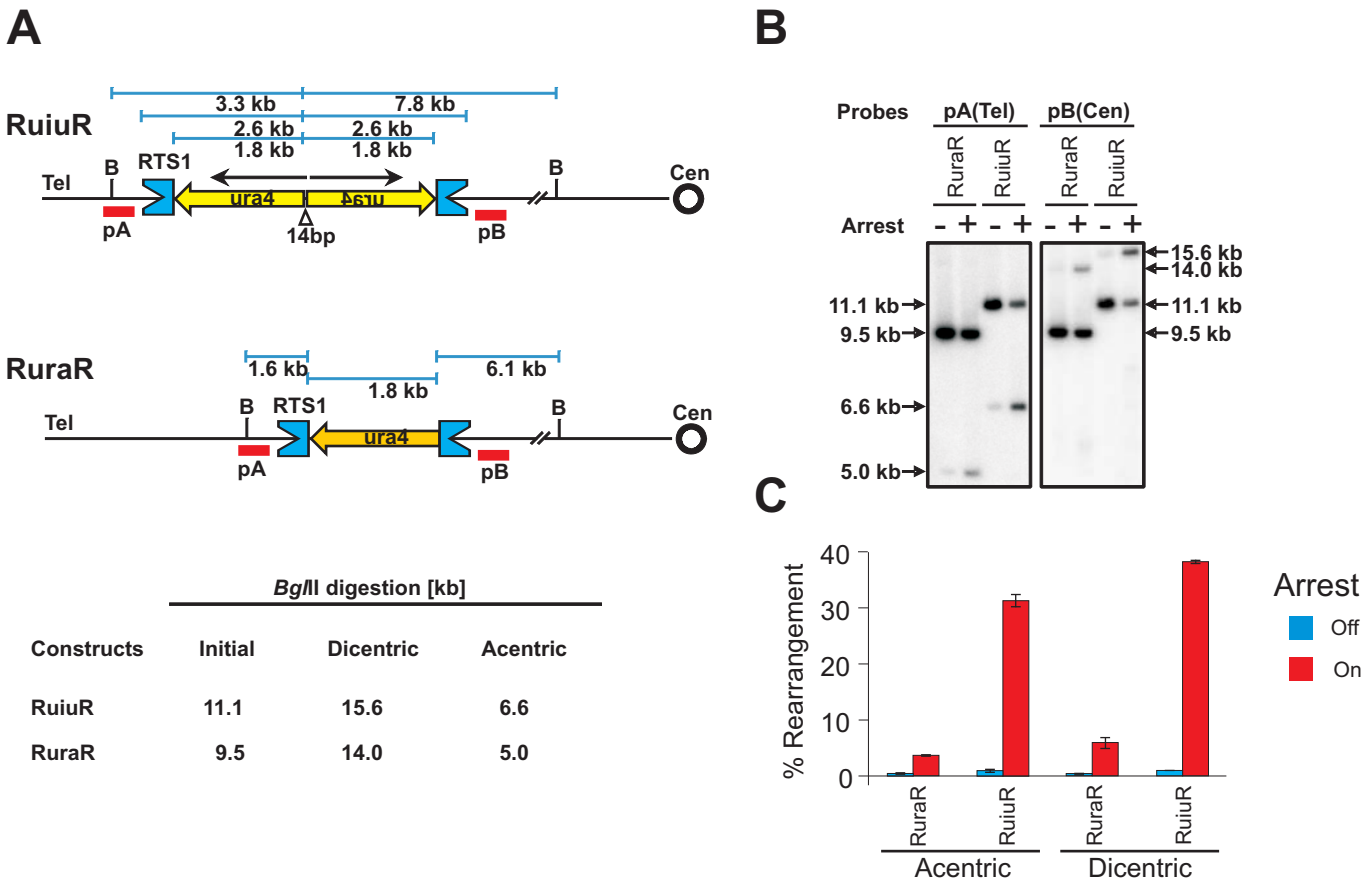

*Bgl*II digestion [kb]

Constructs	Initial	Dicentric	Acentric
RuiuR	11.1	15.6	6.6
RuraR	9.5	14.0	5.0

Figure S2. Rearrangements are increased when replication stalls in a palindrome. (A) Diagrams of RuiuR and RuraR. Open circle indicates centromere cen3. Blue concave, and yellow arrow represent RTS1 and the ura4 gene, respectively. Open triangle shows 14 bps interrupting sequence at the palindrome centre. Red boxes indicates DNA probe. B represents BglII site. Sizes of initial and rearranged BglII fragments of each strains are indicated. (B) Southern blot analyses of RuraR and RuiuR strains for pause off or on. Genomic DNA was digested with BglII and probed with pA or pB. (C) Quantification of the rearranged fragment in (B). Average value and standard deviation of the value are calculated from at least three independent experiments.

Mizuno Supplementary Figure S3.

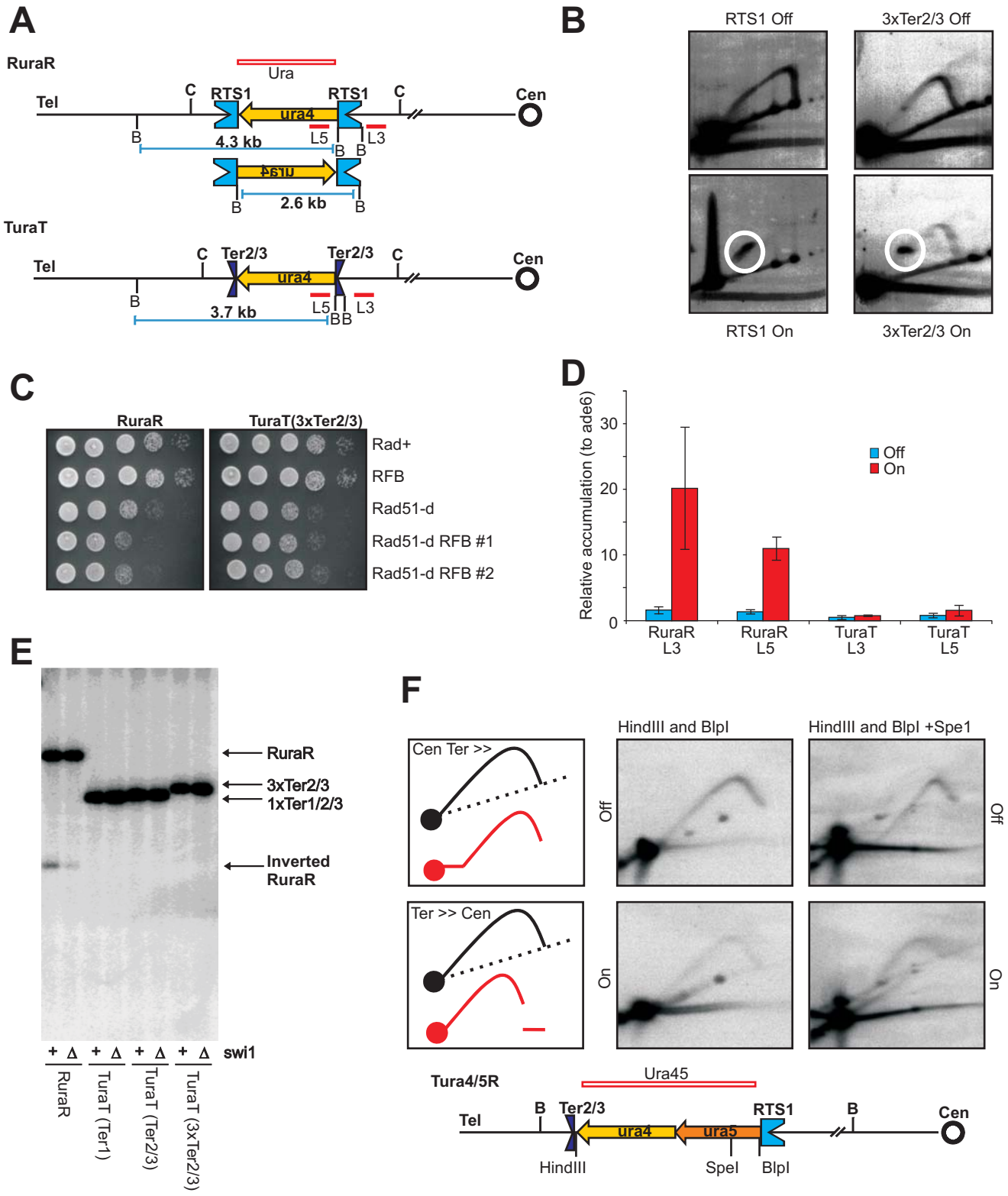

Figure S3. The rDNA replication fork barrier (RFB) Ter2/3 pauses replication forks but does not generate rearrangements and replication restart is not dependent on HR. Consistent with analysis of an ectopic rDNA RFB in S. cerevisiae [Calzada 2005]), cell viability does not depend on Rad51 and Rad52 does not accumulate at the pausing site. (A) Diagrams of RuraR and TuraT (T=3×Ter2/3) represented as in Figure S2A. The constructs were integrated at the ura4 locus on fission yeast chromosome III. Dark concave indicates 3×Ter2/3. C and B show ClaI and BlpI restriction enzyme sites, respectively. Red bars L3 and L5 represent quantitative PCR primer sets for chromatin immunoprecipitation assay and open red box probe Ura. Replication stalling at RuraR leads to a change in orientation of the ura4 gene. This inversion changes the length of the BlpI fragment (RuraR initial length 4.3 kb, inverted length 2.6 kb; TuraT initial length 3.7 kb, predicted inverted length 1.9 kb). (B) Two dimensional agarose (2D) gel analyses of RuraR and TuraT. Both RTS1 and Ter2/3 arrest a replication fork in a Swi1-dependent fashion. The swi1 promoter was replaced with an inducible promoter nmt81 in the strains tested. Replication fork stalling (Pause Off or On) was controlled by turning on or off swi1 transcription. Genomic DNA was digested with ClaI, 2D gel analysis was performed using probe Ura. Note both RTS1 and Ter2/3 arrest replication in a Swi1-dependent manner. (C) Cell viability of RFB strains in a rad51-d background. A serial dilution of culture was spotted on YEA plates and incubated at 30°C for 3days. Note that TuraT does not loose cell viability after induction of replication fork arrest in a rad51-d background, whereas RuraR loses viability. (D) Accumulation of Rad52 at RFB in indicated strains upon induction (Pause On) or repression (Pause Off) of replication fork arrest. Quantitative PCR analysis was performed following chromatin immunoprecipitation of GFP-tagged Rad52. Enrichment of Rad52 is shown (n=3) with the mean value and standard deviation. Note that Rad52 does not accumulate at TuraT even in Pause On. (E) Southern blot analysis of RFB strains with probe Ura. Ter1, Ter2/3, 3×Ter2/3 represents TuraT strains harbouring the indicated rDNA replication fork terminator sequences on both side of the ura4 gene in an inverted repeated manner. All RFBs arrest a replication fork in a Swi1-dependent manner. Genomic DNA was digested with BlpI. Inversion in RuraR changes the BlpI fragment length (Initial length 4.3 kb, inverted length 2.6 kb). Note that no TuraT strain gave a 1.9 kb DNA fragment corresponding to inversion. (F) Direction of replication at the ura4 locus. Below: Diagram of Tura4/5R where 3xTer2/3 and RTS1 flank ura4 and ura5 genes at the ura4 locus. Open circle indicates centromere cen3. Blue concave, dark concave, yellow arrow and orange arrow represent RTS1, 3×Ter2/3, ura4+, and ura5+, respectively. H, S, and B indicate HindIII, SpeI, and BlpI, respectively. Open box shows Probe Ura45. Above: 2D gel analyses of Tura4/5R. The Tura45R strains were grown in rtf1+ (Pause ON) or rtf1-d (Pause Off) backgrounds. Genomic DNA was digested with HindIII and BlpI and run in the first dimension gel. A slice of the gel was treated with or without SpeI digestion and run in the second dimension. Expected migration of DNA fragments is represented on left hand side. Black dot and line show monomer spot and Y-arc without SpeI digestion, whereas red dot and line indicate those with SpeI digestion. The DNA migration pattern depends on the direction of replication. There are two strong replication origins (ARS3004/3005) 5kb centromeric to the ura4 locus. The telomeric origin (ARS3003) is 40kb away and thus in an unperturbed cell the locus will be predominantly replicated from the centromere side. Consistently most of the replication forks come through the ura4 locus from centromere side in the rtf1-d background (Pause off). In contrast the majority of forks come through the ura4 locus from telomere side in Rtf1-expressing cells (Pause on). Comparison of the Y arc signal to monomer spot shows that it is much weaker when Rtf1 is expressed. This is consistent with forks restarted by HR at RTS1 not running as canonical Y intermediates and thus demonstrates significant replication by HR-restarted forks.

Mizuno Supplementary Figure S4.

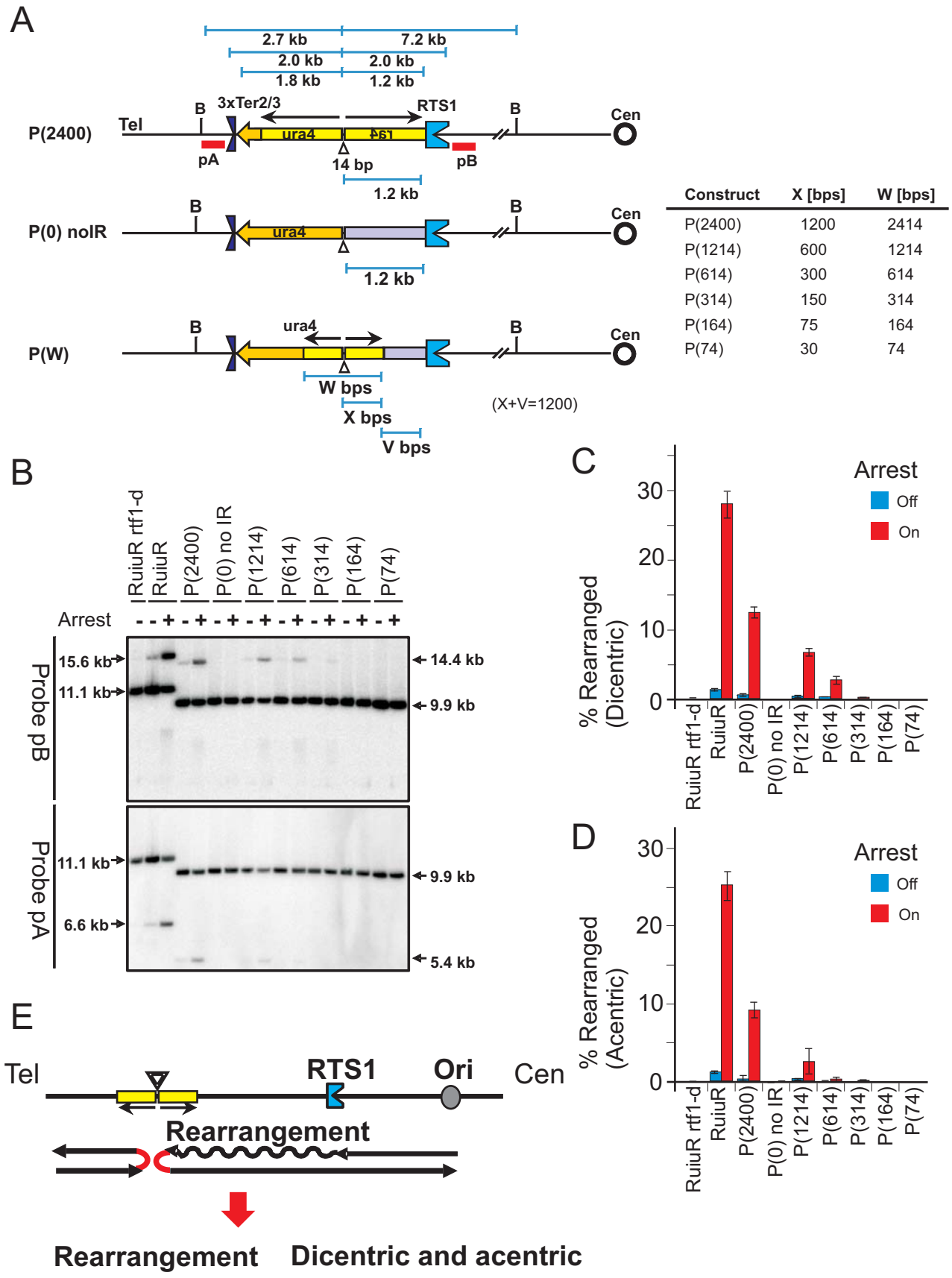

Construct	X [bps]	W [bps]
P(2400)	1200	2414
P(1214)	600	1214
P(614)	300	614
P(314)	150	314
P(164)	75	164
P(74)	30	74

Figure S4. Acentrics and dicentrics are formed with similar frequency dependent on the repeat size. An extended version of Figure 2A-C. A. Cartoon of constructs with varying repeat size. P(2400), P(0)noIR and intermediates [P(W)]. The constructs are indicated as in Figure 1A. W represents the size of the whole palindrome in bps. X shows the size of the ura4 fragment creating the inverted repeat. Grey box indicates heterologous sequence (V). The sum of X and V is always 1200 bps. Probes pB and pA are indicated as red bars. B. Southern blot analyses of P(W) strains for arrest off or arrest on. Genomic DNA was digested with BglII and probed with pB (top) or pA (bottom). Note: top panel is a duplication of Figure 2B. C, D. Quantitation of rearranged fragment in B. Average values and standard deviation are calculated from at least three independent experiments. C and D show per cent of rearranged DNA detected with probes pB and pA, respectively. Note that similar percentages of rearrangements are seen with the two flanking probes indicating that fork U-turns at the centre of the palindrome, which generates a dicentric and also reults in the generation of a reciprocal acentric chromosome, presumably when the tel-proximal fork meets the closed Y. E. Model for generation of acentric and dicentric chromosomes on error-prone progression of a recombination restarted replication fork. Oval, blue concave, and yellow box represent replication origin ARS, obstacle and repeat sequences, respectively. When a replication fork collapses, homologous recombination restarts the collapsed fork. However, the restarted fork is non-canonical and error-prone, causing GCRs at inverted repeats due to executing a U-turn generating a dicentric chromosome. The incoming fork from the other direction is then forced to U-turn generating an acentric chromosome.

Table S1

The *Schizosaccharomyces pombe* strains used in this study

Strains	Genotype	Source/Reference
YKM010	*h⁻ RuiuR sup3.5:nmt41:rtf1 ade6-704 leu1-32*	Mizuno et al., 2009
YKM512	*h⁻ Rpal1R sup3.5:nmt41:rtf1 ade6-704 leu1-32*	This study
YKM515	*h⁻ Rpal2R sup3.5:nmt41:rtf1 ade6-704 leu1-32*	This study
YKM607	*h⁻ smt0 Tpal1R sup3.5:nmt41:rtf1 ade6-704*	This study
YKM610	*h⁻ smt0 Tpal2R sup3.5:nmt41:rtf1 ade6-704*	This study
YKM103	*h⁻ RuiuR rtf1::natMX6 ade6-704 leu1-32*	Mizuno et al., 2009
YKM888	*h⁻ smt0 P(2400) sup3.5:nmt41:rtf1 ade6-704*	This study
YKM893	*h⁻ smt0 P(0)noIR sup3.5:nmt41:rtf1 ade6-704*	This study
YKM896	*h⁻ smt0 P(1214) sup3.5:nmt41:rtf1 ade6-704*	This study
YKM900	*h⁻ smt0 P(614) sup3.5:nmt41:rtf1 ade6-704*	This study
YKM904	*h⁻ smt0 P(314) sup3.5:nmt41:rtf1 ade6-704*	This study
YKM908	*h⁻ smt0 P(164) sup3.5:nmt41:rtf1 ade6-704*	This study
YKM912	*h⁻ smt0 P(74) sup3.5:nmt41:rtf1 ade6-704*	This study
YKM936	*h⁻ smt0 P(1200)IS7 sup3.5:nmt41:rtf1 ade6-704*	This study
YKM940	*h⁻ smt0 P(1200)IS14 sup3.5:nmt41:rtf1 ade6-704*	This study
YKM944	*h⁻ smt0 P(1200)IS28 sup3.5:nmt41:rtf1 ade6-704*	This study
YKM952	*h⁻ smt0 P(1200)IS250 sup3.5:nmt41:rtf1 ade6-704*	This study
YKM947	*h⁻ smt0 P(1200)D0 sup3.5:nmt41:rtf1 ade6-704*	This study
YKM931	*h⁻ smt0 P(1200)D0.6 sup3.5:nmt41:rtf1 ade6-704*	This study
YKM927	*h⁻ smt0 P(1200)D1.2 sup3.5:nmt41:rtf1 ade6-704*	This study
YKM1024	*h⁻ smt0 P(1200)D1.5 sup3.5:nmt41:rtf1 ade6-704*	This study
YKM954	*h⁻ smt0 P(1200)D1.8 sup3.5:nmt41:rtf1 ade6-704*	This study
YKM1027	*h⁻ smt0 P(1200)D2.1 sup3.5:nmt41:rtf1 ade6-704*	This study
YKM1031	*h⁻ smt0 P(1200)D2.4 sup3.5:nmt41:rtf1 ade6-704*	This study
J1162	*h⁻ sup3.5:nmt41:rtf1 RuraR ade6-704 leu1-32*	Lambert et al., 2005
IZM296	*h⁻ ade6-704 leu1-32 RuraR swi1::kanMX6*	This study
SAL117	*h⁻ ade6-704 leu1-32 RuraR*	Lambert et al., 2005
IZM298	*h⁻ ade6-704 leu1-32 TuraT(1xTer1) swi1::kanMX6*	This study
IZM299	*h⁻ ade6-704 leu1-32 TuraT(1xTer2/3) swi1::kanMX6*	This study
IZM300	*h⁻ ade6-704 leu1-32 TuraT(3xTer2/3) swi1::kanMX6*	This study

IZM306	*h⁻ ade6-704 leu1-32 TuraT(1xTer1)*	This study
IZM310	*h⁻ ade6-704 leu1-32 TuraT(1xTer2/3)*	This study
IZM314	*h⁻ ade6-704 leu1-32 TuraT(3xTer2/3)*	This study
IZM321	*h⁻ ade6-704 ura4-D18 leu1-32 rhp51::kan*	This study
IZM338	*h⁺ ade6-704 leu1-32 sup3.5:nmt81:swi1 RuraR*	This study
IZM340	*h⁺ ade6-704 leu1-32 sup3.5:nmt81:swi1 TuraT(3×Ter2/3)*	This study
IZM350	*h⁺ ade6-704 leu1-32 sup3.5:nmt81:swi1 RuraR rad22-GFP::kan*	This study
IZM354	*h⁺ ade6-704 leu1-32 sup3.5:nmt81:swi1 TuraT(3×Ter2/3) rad22-GFP::kan*	This study
IZM383	*h⁻ smt0 ade6-704 leu1-32 rhp51::kan RuraR*	This study
IZM384	*h⁻ smt0 ade6-704 leu1-32 rhp51::kan TuraT(3xTer2/3)*	This study
IZM435	*h⁻ ade6-704 leu1-32*	This study
IZM609	*h⁻ ade6-704 leu1-32 Tura4/5R*	This study
IZM611	*h⁻ rtf1::nat ade6-704 leu1-32 Tura4/5R*	This study